

CDA

COMPETITION BETWEEN FUSION AND QUASI-FISSION IN  
HEAVY ION INDUCED REACTIONS

CONF-8609159--6

DE87 004983

B.B. BACK

Argonne National Laboratory, Argonne, IL 60439-4843, U.S.A.

The submitted manuscript has been authored by a contractor of the U.S. Government under contract No. W-31-109-ENG-38. Accordingly, the U.S. Government retains a nonexclusive, royalty-free license to publish or reproduce the published form of this contribution, or allow others to do so, for U.S. Government purposes.

1. INTRODUCTION

Recently, it has been recognized that complete fusion between heavy ions and heavy targets may be strongly inhibited by dynamical limitations. The strong dissipative forces encountered by the system on the way to the compact shapes necessary for compound nucleus formation reinforce the disruptive coulomb and centrifugal forces leading to an early reseparation into two main reaction products. Depending on the degree of compactness achieved in the intermediate system, varying degrees of mass transfer between the interacting nuclei may have taken place during the reaction. The reaction strength of such binary processes appear to divide into two reasonably well separated channels, namely deeply inelastic scattering and quasi-fission. The former process is characterized by large energy losses approaching the complete damping limit, without any significant net mass transfer, whereas the products of quasi-fission emerges with completely damped kinetic energies and a large net mass flow toward mass symmetry. The general characteristics of these processes are rather well described by recent macroscopic models<sup>1,2</sup>.

The separation of the three main strongly damped processes, complete fusion, quasi-fission and deeply inelastic scattering (see Fig. 1) represents an important experimental challenge. For lighter projectiles,  $A < 35$ , the energy, mass and angular distributions of final fragments from the complete fusion (followed by subsequent fission decay) and quasi-fission reactions are strongly intertwined.

DISCLAIMER

This report was prepared as an account of work sponsored by an agency of the United States Government. Neither the United States Government nor any agency thereof, nor any of their employees, makes any warranty, express or implied, or assumes any legal liability or responsibility for the accuracy, completeness, or usefulness of any information, apparatus, product, or process disclosed, or represents that its use would not infringe privately owned rights. Reference herein to any specific commercial product, process, or service by trade name, trademark, manufacturer, or otherwise does not necessarily constitute or imply its endorsement, recommendation, or favoring by the United States Government or any agency thereof. The views and opinions of authors expressed herein do not necessarily state or reflect those of the United States Government or any agency thereof.

MASTER

DISTRIBUTION OF THIS DOCUMENT IS UNLIMITED

Fig. 1. Schematic illustration of the three different binary reaction channels in strongly damped heavy ion interactions. The present work focusses on the distinction between the compound nucleus fission reaction and the quasi-fission process.

Experimentally based estimates on the relative contribution of the two processes must rely on quantitative analyses of angular distributions<sup>/3,4/</sup> or (if available) angle-mass correlations<sup>/5/</sup>.

For heavier projectiles, the quasifission component becomes more dominant while the complete fusion component subsides. The special characteristics of the complete fusion-fission process in terms of mass independent forward-backward symmetries allows for a quite reliable estimate of this component, even in the presense of much larger quasi-fission contributions. Such methods have recently been applied to measurements of the  $^{238}\text{U} + ^{48}\text{Ca}$  reaction to obtain upper limit estimates of the cross sections for complete fusion near or below the interaction barrier<sup>/5/</sup>. Extrapolating to the systems  $^{48}\text{Ca} + ^{248}\text{Cm}$  and  $^{48}\text{Ca} + ^{254}\text{Es}$  using the well established scaling properties of the extra push model we estimate the cross sections relevant to the efforts of synthesizing super-heavy elements in the region  $Z \sim 116$  and  $N \sim 184$  via heavy-ion fusion reactions. A simple evaporation calculation using properties of the super-heavy elements predicted by Randrup et al.<sup>/6/</sup> shows that the failure to observe super-heavy elements, with the  $^{48}\text{Ca} + ^{248}\text{Cm}$  reaction is consistent with these estimates of the complete fusion cross sections.

## 2. FRAGMENT ANGULAR DISTRIBUTIONS

The estimates of the complete fusion cross sections from the angular distributions of fission-like fragments relies on the assumption of validity of the saddle point model of fission. In this model it is assumed that the angular distribution of fission fragments is given by the nuclear orientation at the saddle point<sup>/7/</sup>. This assumption requires that the axial component,  $K$ , of the total spin,  $I$ , is unchanged during the descent from saddle to scission. The angular distribution may therefore be written

$$W(\theta) \propto \sum_{I=0}^{\infty} (2I+1)T_I \sum_{K=-I}^I \rho(K) |D_{OK}^I(\theta)|^2 \quad (1)$$

where  $T_I$  is the probability for complete fusion and subsequent fission of the  $I$ 'th partial wave,  $\rho(K)$  is the distribution of  $K$ -values at the Saddle point and  $D_{OK}^I$  is the symmetric top rotational wave functions. The problem is now reduced to estimating the  $K$ -distribution at the saddle point. In the statistical model this is a gaussian with a variance<sup>/8/</sup>

$$K_o^2 = \frac{T}{h^2} J_{\text{eff}}; \quad \frac{1}{J_{\text{eff}}} = \frac{1}{J_{\parallel}} + \frac{1}{J_{\perp}} \quad (2)$$

where  $T$  is the nuclear temperature at the saddle point and  $J_{\parallel}$  and  $J_{\perp}$  are the rigid moments of inertia parallel and perpendicular to the symmetry axis, respectively. The shape of the nucleus at the saddle point and the associated moments of inertia may be estimated from e.g. the rotating liquid drop model<sup>/9/</sup> or the Finite Nuclear

It has been found that angular distributions of fission-like products from reactions induced by  $^{19}\text{F}$  or lighter projectiles are rather well accounted for by the saddle point model as outlined above. Heavier projectiles, however, invariably leads to larger anisotropies i.e. smaller  $K_0^2$  values than predicted by this theory<sup>/3,4/</sup>. Measured values (solid points) of  $K_0^2$  are in Fig. 2 compared with the predictions of the rotating liquid drop model (solid curves). The dotted, dashed, and dot-dashed curves represent the predictions of the scission point model under different assumptions of the shape of the system at the scission point<sup>/3,11,12/</sup>. It is apparent that the scission point model is incapable of describing the data, even for the lightest projectiles.

Comparative studies of different entrance channels leading to similar compound systems show that the deviation for the heavier projectiles is more likely to stem from a hindrance of complete fusion than a sudden breakdown of the saddle point theory<sup>/3,4,13/</sup>, i.e. the deviation is clearly associated with a decreasing mass asymmetry in the entrance channel as opposed to the mass of the compound system. This indicates that the increased anisotropy seen with heavy projectiles stems from a contribution of quasi-fission reactions. These may be expected to have larger anisotropies because only more elongated shapes (or smaller K-values) are involved in such reactions. In a quasi-fission reaction one may expect that the distribution of K-values, which initially is a  $\delta$ -function at zero, increases gradually as the the

Fig. 2. Comparison of the experimental values of  $K_0^2$ , obtained from the analysis of the angular anisotropies of fission-like fragments, with the predictions of the saddle point model (solid curves) and the rigid scission point model<sup>/3/</sup> as a function of excitation energy of the fissioning systems. The predictions of the scission point models of Refs. 11 and 12 are represented by the dot-dashed and dotted curves, respectively.

system acquires more compact shapes and experiences particle transfers between the two reaction partners<sup>/14/</sup>. Whether a statistical equilibrium in the axial spin components is achieved during the process is unknown, but the width of the K-distribution would even in this limit be larger than predicted by the saddle point model, since the interaction complex acquires only more elongated shapes during the quasi-fission process.

Based on this observation we may then proceed to disentangle the contributions from true fission of the compound system and the quasi-fission processes, the latter of which do not proceed through the stage of a compound nucleus<sup>/3/</sup>. Such a separation is possible if the individual angular distributions for both compound fission and quasi-fission are known independently. In the analysis it is assumed that the angular distribution of the compound fission component is given by the saddle point model. The angular distribution of the quasi-fission component is, however, less well known. As in Ref. 3 it is assumed that this component has an angular distribution corresponding to a statistical equilibrium at a shape corresponding to an effective moment of inertia  $J_0/J_{\text{eff}} = 1.5$ , where  $J_0$  is the spherical rigid body moment of inertia of the total system. Although this choice is somewhat arbitrary, it has been shown<sup>/3/</sup> that the estimate of the complete fusion cross sections changes only slightly when varying this quantity is changed within reasonable values.

Several macroscopic model calculations<sup>/1,2/</sup> show that there is a distinct fractionation of the two processes in l-space such that the complete fusion reactions preferentially originates from the lowest partial waves, whereas the quasi-fission reactions are associated with higher angular momenta. Under these assumptions one may estimate the complete fusion component by varying the angular momentum which divide the two components such that the observed anisotropy is observed<sup>/3/</sup>.

Complete fusion cross sections estimated in this manner are shown as open triangles in Fig. 3. We observe that the complete fusion accounts for a declining fraction of the total fission cross section as the mass of the projectile is increased. We find, however, that the dynamical hindrance of complete fusion plays a dominating role for projectiles as light as  $^{24}\text{Mg}$  and maybe even  $^{19}\text{F}$ . The consequences of this observation for the prospects of synthesizing super heavy elements using heavy ion fusion reactions may be very far reaching and they will be discussed in detail in the following.

### 3. EXTRA-EXTRA PUSH SYSTEMATICS

The hindrance of complete fusion as observed through the fragment angular distributions may be quantified in terms of an extra-extra push energy required in addition to the interaction barrier energy in order to achieve complete fusion, i.e.

Fig. 3. Comparison of experimental cross sections with theoretical model calculations. Solid circles represent fission cross sections (Refs. 4 and 16 ), open circles are taken from Ref. 17 ( $^{16}\text{O}+^{238}\text{U}$ ), and solid squares represent measurements in which full momentum transfer was required (Refs. 18 and 19). The solid triangles represent the deduced complete fusion cross sections. The cross sections for touching, capture, and complete fusion are shown as solid, dashed, and dashed-dotted curves, respectively<sup>/3/</sup>.

formation of an intermediate complex inside the true fission barrier. A macroscopic model for the interactions between heavy nuclei based on liquid drop model potential energy surfaces and the one-body dissipation mechanism (wall and window formulae) has recently been developed<sup>/1/</sup>. Numerical calculations with this model suggested the following scaling properties for this Extra-Extra Push energy,  $E_{xx}$ , namely

$$E_{xx} = E_{ch} a''^2 [x_m(1) - x_{th}]^2 \quad (3)$$

where  $E_{ch}$  is the characteristic energy of the system and  $x_m(1)$  is the l-dependent mean fissility<sup>/3/</sup>.

Experimental estimates of,  $E_{xx}$ , may be obtained from the ratio of the complete fusion cross section to the cross section for traversing the interaction barrier<sup>/3/</sup>, the latter being obtained from e.g. the proximity potential<sup>/4,15/</sup>. Extrapolating to zero angular momentum one may estimate the the extra-extra push energy for s-waves for the various systems investigated. The scaling properties of the extra-extra push model predicts that the quantity  $(E_{xx}/E_{ch})^{1/2}$  scales linearly with the mean fissility parameter,  $x_m$ , (eq. 3.) as shown in Fig. 4. Because this linear relationship is observed experimentally, one may determine the threshold and strength parameters ,  $x''_{th} = 0.63 \pm 0.03$  and  $a'' = 7 \pm 2$ , from the data. The solid triangles in Fig. 4 represent data points obtained from an analysis of evaporation

Fig. 4. The square root of the extrapolated extra-extra push energy for central ( $l=0$ ) collisions is shown as a function of the mean fissility,  $x_m$ . Data points are based on fission fragment angular distributions, Ref. 4 and references therein. The solid diamond is from the present work.

residue cross sections for Zr and Kr induced reactions<sup>/20/</sup>.

#### 4. MASS-ANGLE CORRELATIONS IN HEAVY SYSTEMS

Recent experiments with  $^{208}\text{Pb}$  and  $^{238}\text{U}$  beams as well as lighter reaction systems have shown that the mass distributions of fission-like fragments have a distinct angular dependence<sup>/19,21-23/</sup>. An example of this is shown in Fig. 5 where the double-differential cross sections are shown as a function of fragment mass and center-of-mass angle, as well as the corresponding angle-integrated mass distributions. These data are taken from Ref. 22. This behaviour is clearly incompatible with a complete fusion - fission process. Such a process would require that the mass distributions are symmetric independent of the scattering angle i.e.

$$\sigma(A, \theta) = \sigma(A_{\text{tot}} - A, \theta) . \quad (4)$$

Furthermore, due to the two-body nature of the fission process, this means that also the angular distributions are forward-backward symmetric for any mass split, i.e.

Fig. 5. Contour diagrams of the double differential cross sections as a function of fragment mass and center of mass scattering angle are shown for binary reactions between  $^{238}\text{U}+^{48}\text{Ca}$  at beam energies of 4.6, 5.9, and 7.5 MeV/u (a). The corresponding angle integrated mass distributions are displayed in panel (b).

$$\sigma(A, \theta) = \sigma(A, \pi - \theta) . \quad (5)$$

We therefore conclude that only a (small) fraction of the fission-like cross section is associated with complete fusion, whereas the quasi-fission process accounts for most of the fission-like strength.

Presently we shall attempt to estimate the complete fusion fraction of the fission-like cross section. Aside from fulfilling the above mentioned obvious requirements, we shall furthermore require that the mass distributions for fission following a complete fusion reaction shall take a gaussian form peaked at symmetry with a variance

$$\sigma_A^2 = T_s/k \quad (6)$$

where  $T_s$  is the nuclear temperature at the scission point and  $k$  is the restoring force constant in the mass asymmetry degree of freedom, taken to be  $k = 0.0035$  MeV/u. The nuclear temperature at scission,  $T_s$ , may be estimated as

$$T_s = \sqrt{(8.5 (E_* + Q_s - E_k)/A)} , \quad (7)$$

where  $E_*$  is the excitation energy of the compound system;  $Q_s$  and  $E_k$  are the ground state Q-value and the total kinetic energy release for symmetric fission, respectively.

As illustrated in Fig. 6. the measured width of the fission mass distribution agrees well with the above estimate for the  $^{238}\text{U}+^{160}\text{O}$ , whereas the reactions with

Fig. 6. The standard deviation of the mass distribution of fission-like products are shown as a function of the excitation at the scission point,  $E^+$ . The thick solid curve is calculated on the basis of Eq. 6. The data are from Ref. 22.

heavier projectiles have increasingly broader mass distributions. This observation supports the earlier conclusion that the quasi-fission process contributes substantially to the fission-like cross section for projectiles heavier than  $^{19}\text{F}$ .

Based on the analysis of fragment angular distributions we furthermore estimate that only ~40% of the cross section at symmetric mass split originates from fission of the compound system. The complete fusion cross section may therefore be estimated as

$$\sigma_{\text{CF}} = 1/2 \sqrt{2\pi} 0.4 \sigma_A \sigma_S \quad (8)$$

where  $\sigma_A$  is given by Eq. 6 and  $\sigma_S$  is the measured angle integrated cross section for symmetric mass split, 40% of which is assumed to originate from compound fission. The factor 1/2 takes into account the multiplicity of symmetric fragments. Estimates of the complete fusion cross sections obtained in this manner are shown as solid squares in Fig. 7 for the  $^{238}\text{U} + ^{48}\text{Ca}$  reaction<sup>/22/</sup>. The cross sections for capture, which are defined as a fully damped process in which a substantial mass drift ( $\Delta A > 10$ ) from the initial mass asymmetry is observed (i.e. complete fusion plus quasi-fission reactions), is plotted as solid points in Fig. 7. We observe that the complete fusion process accounts only for a small fraction of the capture cross section. Indeed, at the lowest energies the complete fusion between  $^{238}\text{U}$  and  $^{48}\text{Ca}$  is hindered by about a factor of 1000.

As for the angular distribution data, the hindrance of complete fusion may at each bombarding energy be expressed in terms of an extra-extra push energy from



which the extra-extra push energy, necessary to achieve complete fusion for s-waves, may be extrapolated. The data point obtained in this way is plotted as a solid diamond in Fig. 3. We observe that this very different way of determining the extra-extra push energy agree's very well with the systematics obtained from the analysis of the fragment angular distributions.

#### 5. CAPTURE AND COMPLETE FUSION CROSS SECTIONS FOR THE $^{238}\text{U}+^{48}\text{Ca}$ REACTION

In Fig. 7 we compare the experimental cross sections for capture and complete fusion for the  $^{238}\text{U}+^{48}\text{Ca}$  reactions with calculations based on the extra-extra push model shown as the solid and the upper dotted curve, respectively. The effects of fluctuations<sup>/24/</sup> in the extra-extra push energy are especially important at the near barrier energies studied for this reaction. We assume that the extra-extra push energy has a gaussian probability function with a variance

$$\sigma_{\text{xx}}^2 = \sigma_0 E_{\text{xx}}, \quad (9)$$

where  $E_{\text{xx}}$  is the average extra-extra push energy and  $\sigma_0$  is a constant which in the present calculation is set to  $\sigma_0 = 2$  MeV. The parameters used in the present

Fig. 7. Experimental capture (solid circles from Ref. 22 and open circles from Ref. 19) and complete fusion (solid squares) cross sections for the  $^{238}\text{U}+^{48}\text{Ca}$  reaction are compared with theoretical calculations represented by solid and dotted curves, respectively. The predicted cross sections for complete fusion (dotted curve) and the (1n), (2n), and (3n) evaporation channels for the  $^{48}\text{Ca}+^{248}\text{Cm}$  reaction in the insert. The experimental<sup>/25/</sup> limit for detecting these products are indicated by open triangles.

calculation are:  $\delta_2 = 0.53$ ,  $\sigma_2 = 0.02$ ,  $a = 8$ ,  $x_{th} = 0.7$ ,  $f = 0.55$ ,  $a'' = 7$ ,  $x''_{th} = 0.63$ ,  $f'' = 0.55$ , and  $\sigma_0 = 2.0$  MeV. The definitions of the parameters are given in Refs. 3, 4, 19.

We find that the extra-extra push model, with these parameters, gives a good representation of the experimental capture and complete fusion cross sections, also in the sub-barrier region. It should be pointed out that the inclusion of fluctuations in the extra-extra push energy is essential for describing the smooth fall-off of the complete fusion cross section for sub-barrier energies. The result is that a non-negligible cross section for complete fusion remains at near or below barrier energies even when a large average extra-extra push energy is needed in order to induce complete fusion for the system. This effect may be essential for the efforts to produce relatively cold super-heavy nuclei by complete fusion reactions.

Encouraged by the consistency with which the extra-extra push model describes the complete fusion cross sections over a wide range of projectile masses, we feel confident in extrapolating to a slightly heavier system, namely the  $^{48}\text{Ca} + ^{248}\text{Cm}$ , which has been used extensively<sup>/25,26/</sup> in attempts to synthesize and detect the superheavy element  $Z=116$ . The predicted complete fusion cross section for this reaction is shown as the lower dotted curve in Fig. 7. We find that complete fusion cross sections in excess of the upper limits of about  $10^{-6}$  mb established by recent experiment<sup>/26/</sup> are predicted for center-of-mass energies down to  $E_{c.m.} = 178$  MeV, which is far below the interaction barrier of  $V_{int} = 201$  MeV. Although it should be kept in mind that these estimates probably represent upper limits, it appears that one should consider the survivability of the super heavy element as responsible for the negative result of these searches.

## 6. SURVIVABILITY AND DETECTABILITY OF SUPER-HEAVY ELEMENTS

A successful synthesis and identification of a super-heavy element depends on three factors. These are: 1) the cross section for the formation of a super-heavy compound system in e.g. a heavy-ion fusion process, 2) the survivability of this compound system against fission decay in the de-excitation process and 3) the half-life and main decay branch of the resulting nucleus. The present work is mainly concerned with the first of these factors, namely an estimate of the complete-fusion cross section. After finding that this estimate exceeds the upper limits set by experiments for the production cross section, it is, however, of interest to determine whether theoretical predictions of the survivability and stability of the super-heavy element would explain the negative results of these searches.

There has been a number of theoretical predictions of the stability of nuclei in the super-heavy region, all of which are based on the Strutinski<sup>/27/</sup> procedure for calculating the stabilizing effect of the nuclear shell structure. Such

calculations have been carried out with different nuclear potentials, shape parametrization and characteristics of the underlying average properties. Depending on the details of such calculations, estimates of the lifetimes which differs by as much as fifteen orders of magnitudes have been obtained<sup>/6,28-31/</sup>. Since the earliest predictions of stable super-heavy elements were made and as increasingly sophisticated experiments lowered the cross section and half-life limits for their production and stability, respectively, it has become clear the most optimistic of these predictions must almost certainly be wrong and that the more pessimistic ones are closer to reality.

In order to estimate the survivability of a  $Z=116$  nucleus formed by complete fusion between  $^{48}\text{Ca}$  and  $^{248}\text{Cm}$  we have chosen to use properties predicted by Randrup et al.<sup>/6/</sup>. These belong to the more pessimistic predictions of super-heavy element stability. Predicted ground state masses, fission barriers and neutron binding energies are used in an evaporation calculation using the monte carlo computer code LSPACE<sup>/32/</sup>. The experimental searches have been carried out in the energy range  $E_{c.m.} = 180-210$  MeV, where we expect one to three neutrons to be emitted before reaching the ground state. The calculated survival probabilities are quite substantial, leading to cross sections above the experimental upper limits. This is, however, consistent with experimental findings, since the residual nuclei after the evaporation of one to three neutrons are predicted to have half-lives much shorter than needed for positive identification, see Table 1. Furthermore, fission is the main decay channel, which would also impair a positive identification, see Fig. 8.

The results of very recent calculations of Moller et al.<sup>/31/</sup> are also listed in table 1. These calculations give a very good description of the masses of the heaviest nuclei, which have recently been discovered. Estimates of the fission barrier heights and the fission half-lives are not available in this case. As is case for the Randrup calculations<sup>/6/</sup>, we may, however, assume that the height of the fission barrier approximately matches the shell energy  $\Delta E_{\text{shell}}$  also in the Moller calculations. This means that fission barriers roughly in the range  $B_f = 7.7 - 8.4$  MeV are predicted in this case, leading to the a larger survivability against fission. This would result in evaporation residue cross sections well above the detection threshold. The predicted partial half-lives for alpha-decay are, however, only slightly higher than the limit for detection. The failure to observe evaporation residues in the extensive searches using the  $^{48}\text{Ca} + ^{248}\text{Cm}$  reaction is therefore not at variance with these predictions.

## 7. THE $^{48}\text{Ca} + ^{254}\text{Es}$ REACTION

Recently, it has been proposed to produce a target of  $^{254}\text{Es}$  of sufficient thickness to carry out experiments with the  $^{48}\text{Ca} + ^{254}\text{Es}$  reaction<sup>/33/</sup>. The virtue of using this reaction is that it leads to product nuclei with a neutron number very

Fig. 8. The predicted<sup>/6/</sup> halflives of various isotopes of the 116'th (solid circles) and the 119'th element (open circles) are shown as a function of neutron number. The predominant decay mode of each nucleus is indicated.

close to the predicted tightly bound  $N=184$  neutron shell. In Fig. 9 we show predictions of the complete fusion cross section (dotted curve) for this system based on the extra-extra push systematics discussed in Sect. 3. The solid curves represent the predicted cross sections for evaporation residues for this system based on the masses and fission barriers predicted by Randrup et al.<sup>/6/</sup>. The residual nucleus after the evaporation of one neutron is predicted to decay preferentially by alpha-emission with a half-life of  $T_{1/2} = 30$  ms, which is far above the experimental limit of about 1  $\mu$ s. Taking these predictions at face value, the complete fusion reaction  $^{48}\text{Ca} + ^{254}\text{Es}$  appears to be a good candidate for super-heavy element synthesis if studied at a center-of-mass energy in the range  $E_{\text{c.m.}} = 190\text{-}200$  MeV where the (ln) reaction is predicted to peak.

On the other hand, if one considers the calculations of Moller et al.<sup>/31/</sup>, a quite different picture emerges. These authors predict that the final products of this reaction are very unstable against alpha-decay, with half-lives in the ns region, which is beyond the reach of present detection techniques.

The case for the  $^{48}\text{Ca} + ^{254}\text{Es}$  reaction may therefore be summarized as follows. Some theoretical predictions are sufficiently optimistic for the finally obtaining the elusive goal of synthesizing a super-heavy element, that experimentalists are tempted to pursue this reaction. On the other hand, there is a different calculation which will be able to explain a possible negative result of such an effort. This situation is not unusual in science, and hopefully, it will

Fig. 9. The predicted complete fusion (dotted curve), and the (1n), (2n), and (3n) cross sections (full drawn curves) are compared with experimental sensitivities.

not restrain experimentalists from probing the upper limits of the periodic table.

## 8. SUMMARY AND CONCLUSIONS

The distinction between complete fusion, followed by fission decay, and quasi-fission reactions may be somewhat elusive because there is no clean separation of the two processes in observable quantities, such as energy, emission angle or mass of the final fragments. For the prospects of synthesizing super-heavy elements this distinction is very real, because only the complete fusion reaction may lead to the formation of a (semi-) stable nucleus in the ground state, which contains all of the nucleons of the target and the projectile (except for a few evaporated neutrons). Since complete fusion is the most promising reaction for achieving synthesis of super-heavy elements from the available target and projectile species, it is of importance to study and obtain a better understanding of the competition between complete fusion and quasi-fission reactions.

In the present paper we present a study of the relative importance of complete fusion and quasifission processes based on two different observations. In one approach the deviation of the measured anisotropy of fission-like fragments from theory is interpreted as a contribution of quasi-fission processes, the strength of which is estimated by a quantitative analysis of this deviation. The resulting estimates of the relative contribution of complete fusion and quasi-fission

reactions is shown to follow the scaling properties of the extra-extra push model. Secondly, the mass-angle correlation of binary fragments from the  $^{238}\text{U} + ^{48}\text{Ca}$  reactions is studied in order to estimate the contribution from complete fusion processes, which are assumed to display characteristics in accordance with the fission decay of lighter compound systems. Also in this case does the competition between the two competing processes follow the scaling properties of the extra-extra push model.

Encouraged by the success in accounting for the complete fusion component in lighter systems we proceed to calculate the complete fusion cross section for the reactions  $^{48}\text{Ca} + ^{248}\text{Cm}$  and  $^{48}\text{Ca} + ^{254}\text{Es}$ . According to these calculations we find that, although a strong inhibition of the complete fusion process is expected for these systems, the cross section for complete fusion is predicted to be sufficient large to hope that synthesis of super-heavy elements may be possible.

Although a careful search for super-heavy elements using the  $^{48}\text{Ca} + ^{248}\text{Cm}$  has been carried out in several laboratories, such efforts have been fruitless so far. Based on theoretical calculations<sup>/6,31/</sup> it is argued that the instability of the evaporation residues rather than the inhibition of the complete fusion process is responsible for the negative result.

The situation is less clear for the  $^{48}\text{Ca} + ^{254}\text{Es}$  reaction, which has recently been proposed as a candidate for super-heavy element synthesis<sup>/33/</sup>. Again we predict that the complete fusion process, although strongly suppressed, is of sufficient strength for the formation of detectable number of compound nuclei. The predictions of the stability of the evaporation residues diverges rather strongly, casting a shadow of doubt on the prospects for detecting super-heavy elements with this reaction.

This research was supported by the U. S. Department of Energy, Nuclear Physics Division, under Contract W-31-109-Eng-38.

## References

1. W.J.Swiatecki, Phys. Scr. 24, 113 (1981); W.J.Swiatecki and S.Björnholm, Nucl. Phys. 391, 471 (1982).
2. H.J.Feldmeier, Argonne Report, ANL-PHY-85-2 (1985).
3. B.B.Back, Phys. Rev. C32, 2104 (1985); *ibid.* Phys. Rev. C32, 1786 (1985).
4. B.B.Back et al. Phys. Rev. C33, 195 (1985); *ibid.* Phys. Rev. C33, 385 (1986).
5. B.B.Back et al., submitted to Z. Phys. (July 1986).
6. J.Randrup et al., Phys. Scr. 10A, 60 (1974).
7. Aage Bohr, in Proceeding sof the united Nations International Conference on the Peaceful Uses of Atomic Energy, Geneva, Switzerland, 1955 (United Nations, New York, 1956), Vol. 2, p. 151.
8. I.Halpern and V.M.Strutinski, in Proceedings of the Second United Nations International Conference on the Peaceful Uses of Atomic Energy, (United Nations, Geneva, Switzerland, 1958), p. 408.
9. S.Cohen, F.Plasil and W.J.Swiatecki, Ann. Phys. (N.Y.) 82, 557 (1974).
10. A.J.Sierk, Phys. Rev. C33, 2039 (1986).
11. P.Bond, Phys. Rev. Lett. 52, 414 (1984) ; P.Bond, Phys. Rev. C32, 471 (1985).

12. H.H.Rosner, J.R.Huizenga, and W.U.Schröder, Phys Rev. Lett. 53, 38 (1984).
13. B.B.Back et al., Phys. Rev. Lett. 50, 818 (1983).
14. T.Dossing and J.Randrup, Nucl. Phys. A333, 215 (1985).
15. J.Blocki et al., Ann. of Phys. 105, 477 (1977).
16. M.B.Tsang, H.Utsunomiya, C.K.Gelkbke, W.G.Lynch, B.B.Back, S.Saini, P.A.Baisden, and M.A.McMahan, Phys. Lett. B129, 18 (1983).
17. V.E.Viola, Jr. and T.Sikkeland, Phys. Rev. 128, 767 (1962).
18. A.Gavron et al., Phys. Rev. C30, 1550 (1984).
19. J.Töke et al., Nucl. Phys. A440, 327 (1985).
20. C.-C.Sahm et al., Z. Phys. 319, 113 (1984).
21. R.Bock et al., Nucl. Phys. A388, 334 (1982).
22. W.Q.Shen et al., Europhys. Lett. 1, 113 (1986); W.Q.Shen, to appear.
23. B.B.Back et al., Proceedings of the Conference on the Many Facets of Heavy Ion Fusion Reactions, Argonne, March 24-26, 1986.
24. C.-C. Sahm et al., Nucl. Phys. A441, 316 (1985).
25. Yu. Ts. Oganessian et al., Nucl. Phys. A294, 213 (1978).
26. P.Armbruster et al., Phys. Rev. Lett. 54, 406 (1985).
27. V.M.Strutinski, Yad. Fiz. 3, 614 (1966) [Sov. J. Nucl. Phys. 3, 449 (1966)]; V.M.Strutinski, Nucl. Phys. A95, 420 (1967).
28. S.G.Nilsson et al., Nucl. Phys. A131, 1 (1969).
29. M.Brack et al., Rev. Mod. Phys. 44, 320 (1972).
30. E.O.Fiset and J.R.Nix, Nucl. Phys. A193, 647 (1972).
31. P.Möller G.A.Leander, and J.R.Nix, Z. Phys. A323, 41 (1985); and P.Möller, private communication (1985).
32. A.Gavron, Phys. Rev. C21, 230 (1980); Y.Eyal and M.Hillman, Evaporation Code JULIAN (unpublished).
33. A.Ghiorso et al., LBL Report PUB-5118 (April 1984).

**Table 1:** Predicted Properties of Super-Heavy Elements

Nucleus			Randrup et al. <sup>/6/</sup>				Möller et al. <sup>/31/</sup>		
Z	A	xn	$\Delta E_{\text{shell}}$ (MeV)	$B_f$ (MeV)	$B_n$ (MeV)	$\log(T_{1/2}/y)^a$	$\Delta E_{\text{shell}}$ (MeV)	$B_n$ (MeV)	$\log(T_\alpha/y)^b$
116	296	on	-5.9	5.7	7.7	-10	-7.7	6.3	-13.8
116	295	1n	-5.2	4.9	6.3	-14	-8.4	5.6	-11.8
116	294	2n	-4.5	4.1	7.9	-17	-8.4	7.3	-12.3
116	293	3n	-3.8	3.3	6.4	-22	-8.3	6.0	-11.8
119	302	on	-7.9	7.8	6.5	-8.7	-5.8	5.7	-15.1
119	301	1n	-7.1	7.0	7.8	-9.1	-6.0	6.7	-15.9
119	300	2n	-6.4	6.0	6.6	-11	-6.5	5.7	-16.0
119	299	3n	-5.8	5.3	8.1	-14	-6.8	6.7	-13.2

a) Total half-lives, main decay modes are indicated in Fig. 8.

b) Alpha half-lives only.

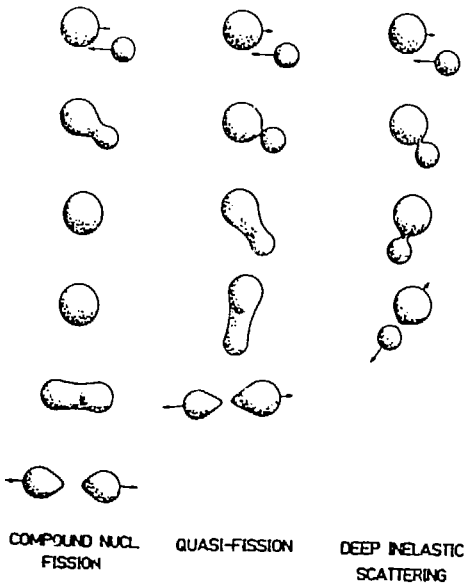


Fig. 1

Fig. 1



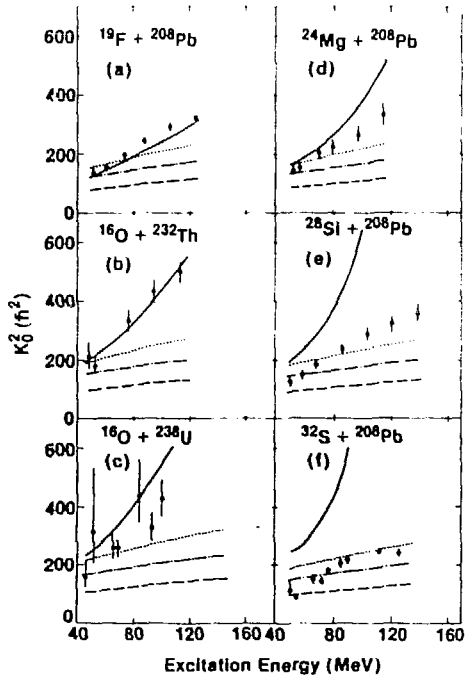


Fig. 2

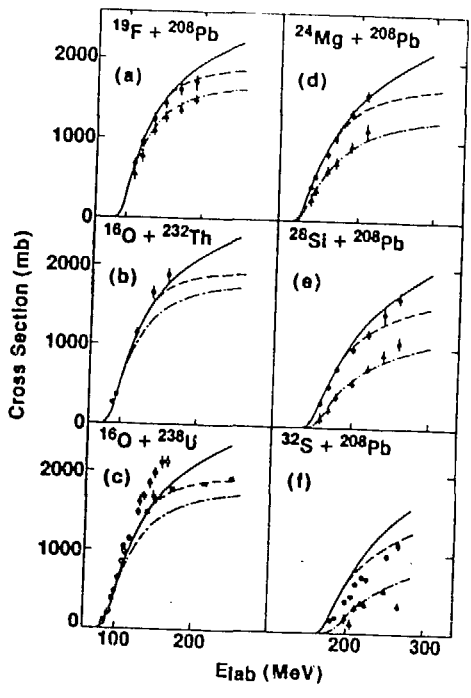


Fig 3

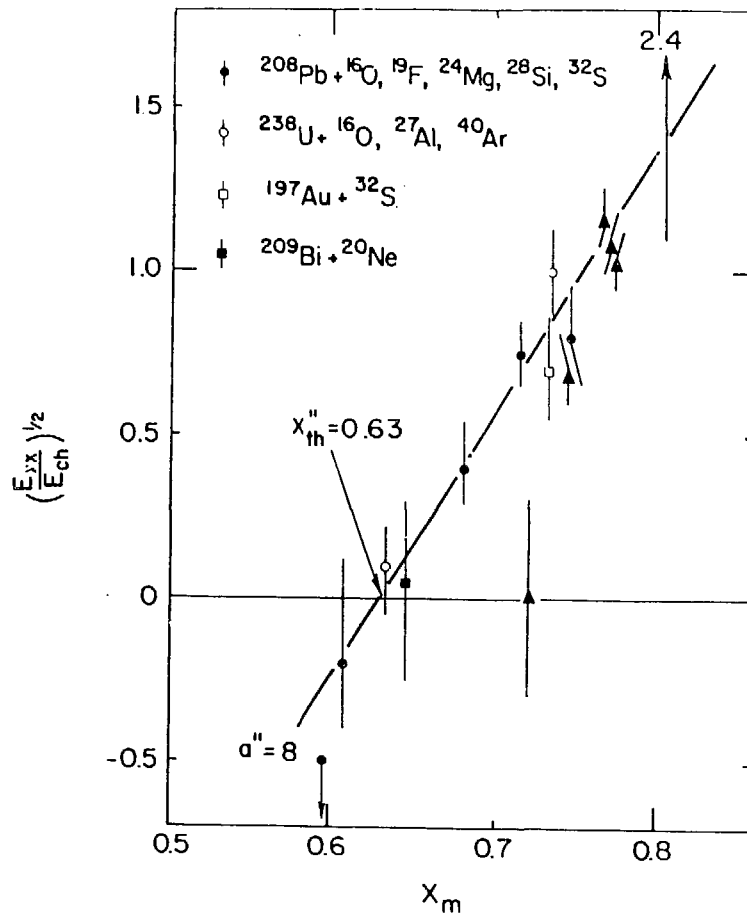


Fig. 4

Not find.

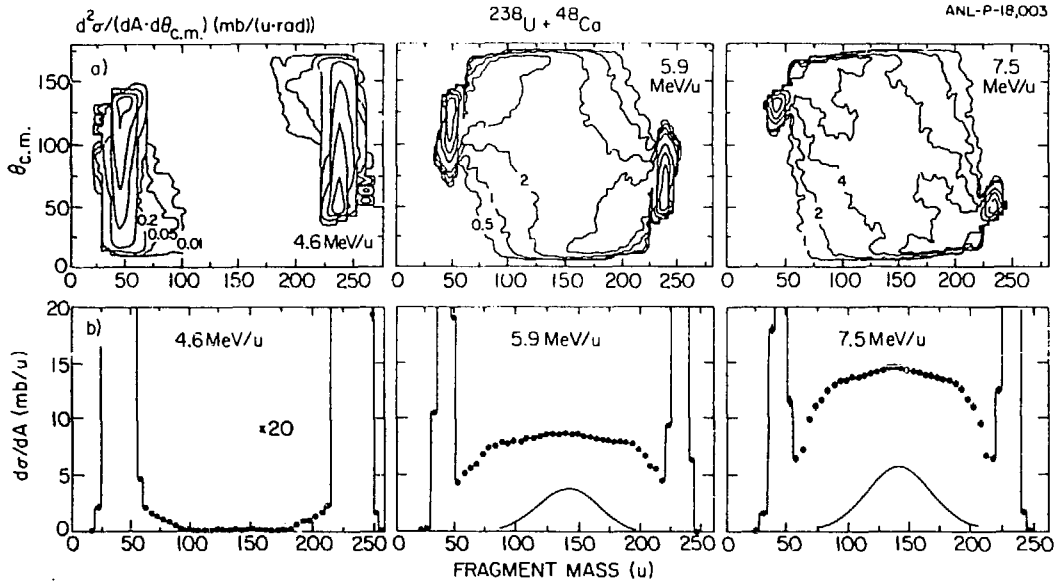


Fig. 5

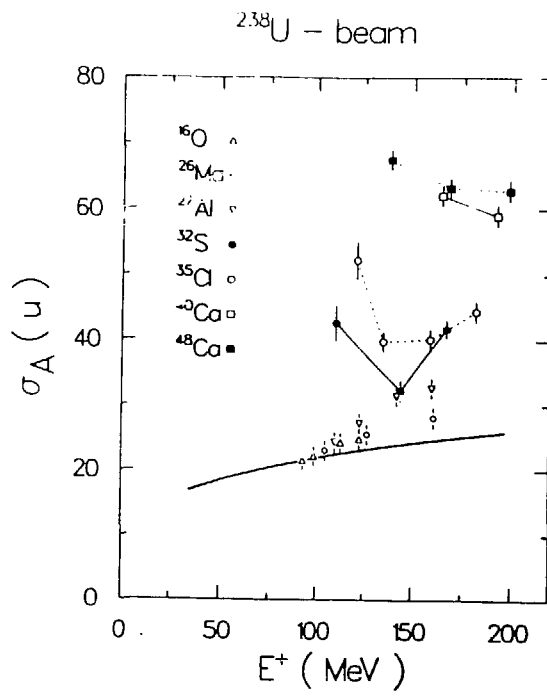


Fig. 6

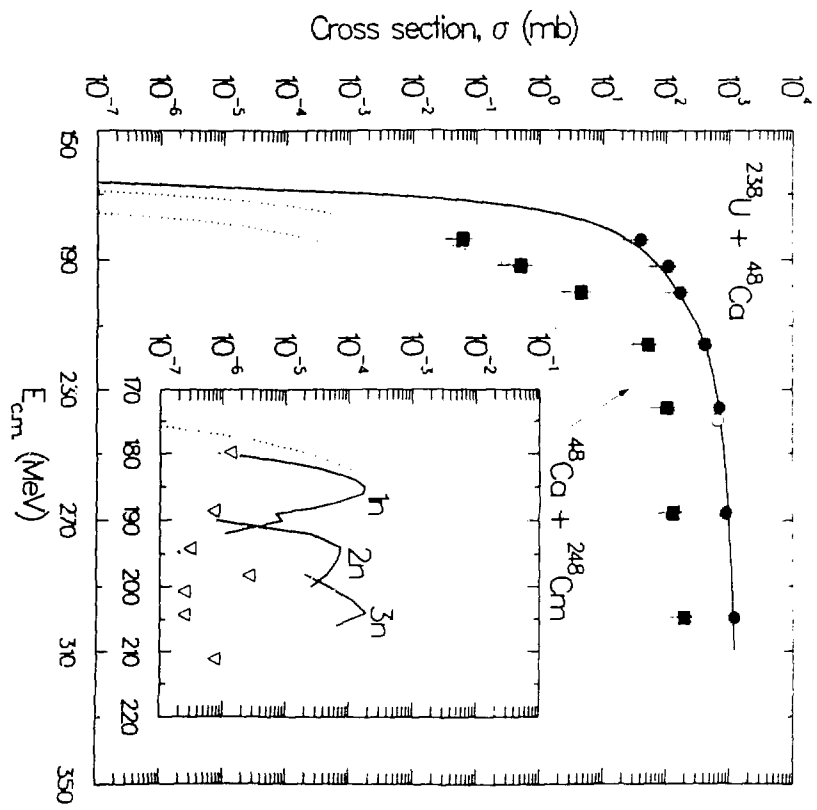


Fig 7

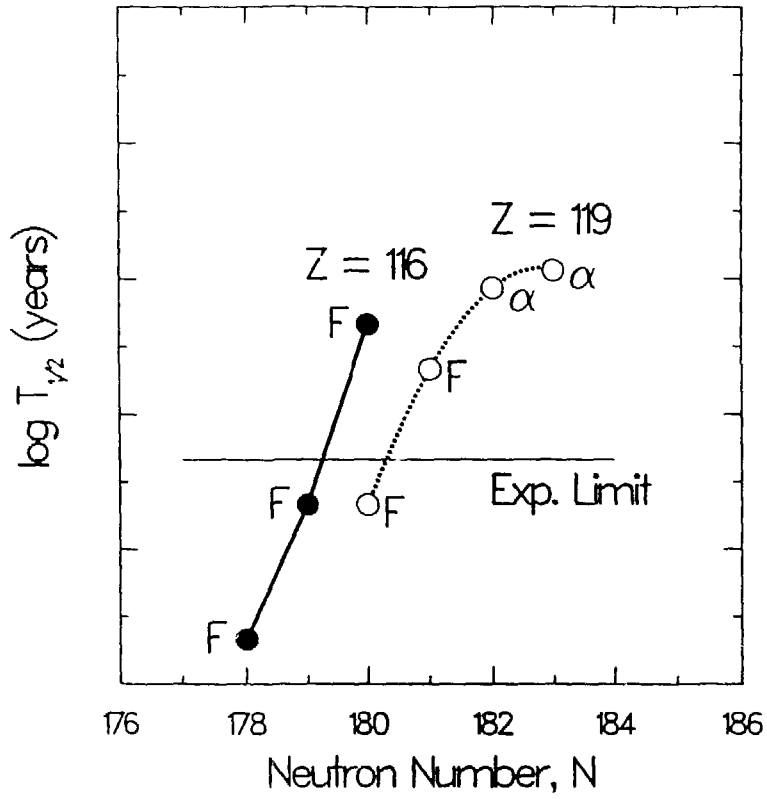


Fig 8

Not final.

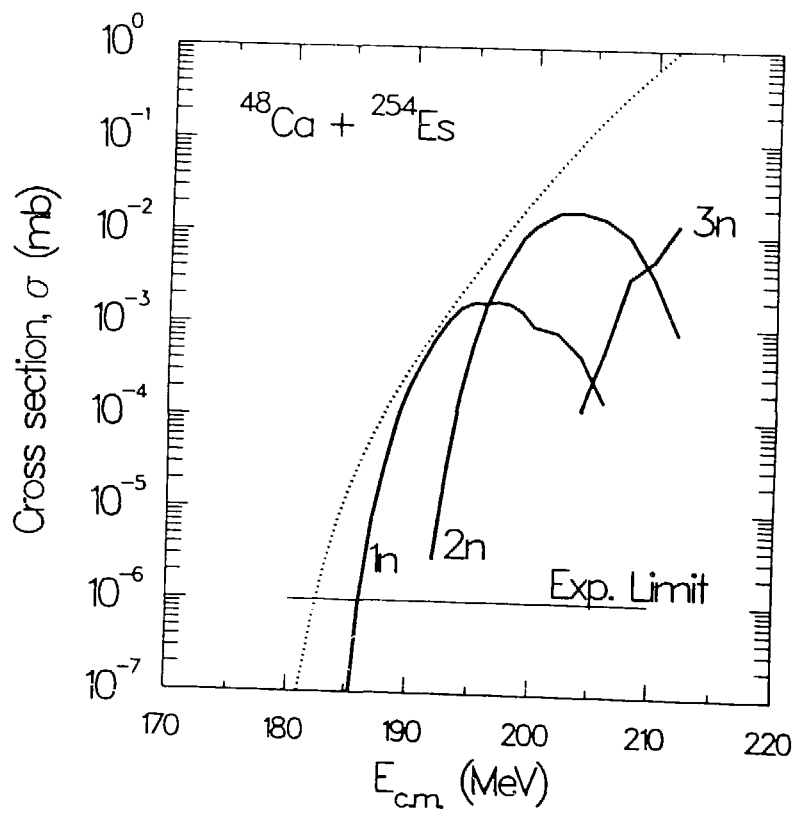


Fig. 9.